THEORETICAL AND APPLIED MECHANICS

Volume 24

Proceedings of the 24th Japan National Congress for Applied Mechanics, 1974

Edited by Japan National Committee for Theoretical and Applied Mechanics Science Council of Japan

UNIVERSITY OF TOKYO PRESS

Non-Linear Vibration Analysis of Plane Framed Structures by Finite Element Method

Yukio MAEDA, Masa HAYASHI and Ken-ichi MAEDA

Department of Civil Engineering, Osaka University, Suita-city

In recent years, the finite element method has been extensively developed for solving structural problems on the dynamic response of structural systems with material and geometrical nonlinearities.

In this paper, four different procedures are newly proposed or reviewed for solving non-linear equations of motion by piecewise linearization. Although these procedures described herein are restricted to the geometrically non-linear vibration analysis of plane framed structures, extended use of their basic algorithms may be possible in the field of material nonlinearities and even in that of three-dimensional problems.

For justification of the methods proposed, the results of some numerical calculations are presented and compared with the ones obtained by the Newton-Raphson iteration.

I. INTRODUCTION

Recent developments of high-speed digital computers and numerical analysis techniques have enabled the finite element method even to find frequent application in the non-linear vibration analysis of structural systems with material and geometrical nonlinearities. An analytical solution of non-linear equations of motion is apparently introduced by a pure iteration method for solving non-linear differential equations. This method, however, requires a great number of iterations, and a lengthy operating time, at every time step in a numerical integration. For this reason, the demand for reduction of an operating time, has drawn attention of many investigators.

Piecewise linearization[1–6] is one of the powerful method to answer the question. In this technique, the equations of motion is formulated on the incremental basis by using a linearized stiffness corresponding to conditions at the beginning of each time step in a numerical integration. Consequently, it should be noted that the amount of time-increment must be smaller than a value needed to prevent excess accumulation of numerical errors due to linearization of a non-linear stiffness as well as truncation errors due to interpolation of an inertia force. Namely, the degree of accuracy of the linearized stiffness, approximated at each incremental time step, is the most closely related to rational reduction of an operating time. Many reports on this type of study have been published up to date. Particularly, the study done by J. H. Argyris et al.,[1] in which high accuracy in the piecewise linearization was achieved by use of a modified stiffness matrix instead of a tangential stiffness, is worth noting. On the other hand, if an incremental form of the equations of motion enables the application of a mode superposition besides a direct integration, the procedure is expected to display its ability in some cases, as a quick and convenient method although incompletely accurate. The study made by Nickel, R. E.[5] is one of its representative examples.

From the above discussions, in this paper four different procedures are newly proposed

or reviewed for solving the non-linear equations of motion by piecewise linearization. Although these procedures described herein are restricted to the geometrically non-linear vibration analysis of plane framed structures, extended use of their basic algorithms may be possible in the field of material nonlinearities and even in that of three-dimensional problems.

For justification of the methods proposed, the results of some numerical calculations are presented and compared with the ones converged by the Newton-Raphson iteration at every incremental time step. As numerical analysis techniques for a step-by-step integration and for an eigen-value problem expressed in terms of large order banded matrices, the well-known Newmark's β-method[7,8] and the combined Sturm sequence method by K. K. Gupta[9] are adopted, respectively. Finally, from all the results, general features of the non-linear vibration analysis of plane framed structures by the finite element method are discussed.

II. NON-LINEAR EQUATIONS OF MOTION

The non-linear equations of motion of a discretized continuum express an equilibrium among dynamic forces with respect to system coordinates and time t. Thus, if an inertia force is expressed in terms of the product of a nodal acceleration vector $\ddot{X}(t)$ and a constant mass matrix M, the form may be written by neglecting damping force as:

$$R(X(t)) = F(t) - M \cdot \ddot{X}(t) \tag{1}$$

where $R(X(t))$ is an iternal resisting force vector, considered to include the terms higher than the second order of a nodal displacement vector $X(t)$, and $F(t)$ is an externally applied force vector.

III. INITIAL INTERNAL RESISTING FORCE VECTOR AND CHORDAL STIFFNESS MATRIX

It should be assumed that each member of a plane framed structure is straight and has a uniform section, and then the relation between stresses and strains is linear.

With axial and transverse displacements, u and v, in a member coordinates, an initial strain ε under an initially deformed state and its increment $\Delta\varepsilon$ are given by Eq. (2), corresponding to a usual large-deformation analysis:

$$\left.\begin{aligned} \varepsilon &= u_x + \frac{1}{2} v_x^2 - y \cdot v_{xx}, \\ \Delta\varepsilon &= \Delta u_x + \frac{1}{2} \Delta v_x^2 - y \cdot \Delta v_{xx} + v_x \cdot \Delta v_x \end{aligned}\right\} \tag{2}$$

where subscripts of u, v, Δu and Δv represent differentiation by x in the direction of the member axis.

Then, the increment ΔU of the member's initial strain energy U is given as follows:

$$\Delta U = E \cdot \int \left(\varepsilon \cdot \Delta\varepsilon + \frac{1}{2} \Delta\varepsilon^2 \right) dV$$

$$= \delta U + \delta^2 U + E \cdot \int \left\{ \frac{1}{2} \left(\Delta u_x \cdot \Delta v_x^2 + \frac{1}{4} \Delta v_x^4 \right) + \frac{1}{2} v_x \cdot \Delta v_x^3 \right\} dV \tag{3}$$

where δU and $\delta^2 U$ are the first and second variations of U, respectively.

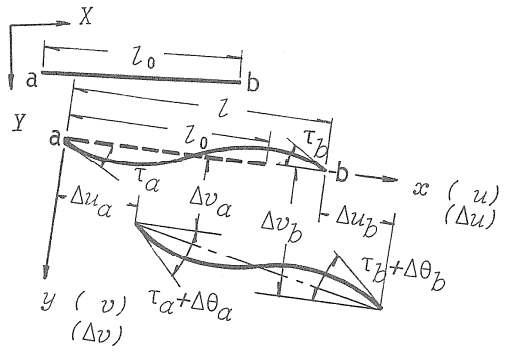

Fig. 1. End-displacements of member.

Now, on the well-established principle of the finite element method, it is necessary to introduce shape functions. To completely exclude a rigid-body displacement of a member from a value of the initial strain, the forms of Eq. (4), with the notations illustrated in Fig. 1, are newly suggested in this paper and adopted:

$$\left.\begin{aligned}
u &= \frac{x}{l_0} \cdot (l - l_0), \\
v &= \left(x - \frac{2x^2}{l_0} + \frac{x^3}{l_0^2} \right) \cdot \tau_a + \left(-\frac{x^2}{l_0} + \frac{x^3}{l_0^2} \right) \cdot \tau_b, \\
\Delta u &= \left(1 - \frac{x}{l_0} \right) \cdot \Delta u_a + \frac{x}{l_0} \cdot \Delta u_b, \\
\Delta v &= \left(1 - \frac{3x^2}{l_0^2} + \frac{2x^3}{l_0^3} \right) \cdot \Delta v_a + \left(x - \frac{2x^2}{l_0} + \frac{x^3}{l_0^2} \right) \cdot \Delta\theta_a \\
&\quad + \left(\frac{3x^2}{l_0^2} - \frac{2x^3}{l_0^3} \right) \cdot \Delta v_b + \left(-\frac{x^2}{l_0} + \frac{x^3}{l_0^2} \right) \cdot \Delta\theta_b
\end{aligned}\right\} \tag{4}$$

where l_0 and l are a non-stress length of a member and its initially deformed one, respectively.

Consequently, the increment ΔU of the strain energy, given by Eq. (3), can be expressed as the function of an initial end-displacement vector $\boldsymbol{u}(0, 0, \tau_a, l-l_0, 0, \tau_b)$ and its increment $\Delta\boldsymbol{u}(\Delta u_a, \Delta v_a, \Delta\theta_a, \Delta u_b, \Delta v_b, \Delta\theta_b)$ in the member coordinates under the initially deformed state.

The equations to connect an end-load vector to an end-displacement one at the end of the incremental step may be derived by the stationary condition of potential energy as:

$$\begin{aligned} \boldsymbol{p} + \Delta\boldsymbol{p} = & \{\boldsymbol{k}_0 + \boldsymbol{k}_1(\boldsymbol{u}) + \boldsymbol{k}_2(\boldsymbol{u}^2)\} \cdot \boldsymbol{u} + [\{\boldsymbol{k}_0 + 2\boldsymbol{k}_1(\boldsymbol{u}) + 3\boldsymbol{k}_2(\boldsymbol{u}^2)\} \\ & + \{\boldsymbol{k}_1(\Delta\boldsymbol{u}) + \boldsymbol{k}_2(\Delta\boldsymbol{u}^2)\} + \boldsymbol{k}_{11}(\boldsymbol{u}, \Delta\boldsymbol{u})] \cdot \Delta\boldsymbol{u} \\ = & \boldsymbol{k}(\boldsymbol{u}) \cdot \boldsymbol{u} + \tilde{\boldsymbol{k}}(\boldsymbol{u}, \Delta\boldsymbol{u}) \cdot \Delta\boldsymbol{u} \end{aligned} \tag{5}$$

where $\boldsymbol{p}$ and $\Delta\boldsymbol{p}$ are an initial end-load vector and its increment, respectively. Except that parameters are qualitatively different from the previous ones, matrices $\boldsymbol{k}_1$ and $\boldsymbol{k}_2$ are the usual first and second non-linear stiffness matrices, respectively. Matrix $\boldsymbol{k}_{11}(\boldsymbol{u}, \Delta\boldsymbol{u})$ is shown in Appendix.

From the characteristics of the shape functions adopted in this paper, it is evident that:

$$\boldsymbol{p} = \boldsymbol{p}(\boldsymbol{u}) = \boldsymbol{k}(\boldsymbol{u}) \cdot \boldsymbol{u}. \tag{6}$$

Hence, if the initial end-displacement vector $\boldsymbol{u}$ of the member is calculated corresponding to an initial nodal displacement vector $X(t)$, an initial internal resisting force vector $R(X(t))$ can be easily evaluated by summarizing the initial end-load vector $\boldsymbol{p}(\boldsymbol{u})$ of all the members, as multiplied by each coordinate transformation matrix $\boldsymbol{c}(X(t))$.

Moreover, Eq. (5) may be rewritten from the above consideration as

$$\Delta\boldsymbol{p} = \tilde{\boldsymbol{k}}(\boldsymbol{u}, \Delta\boldsymbol{u}) \cdot \Delta\boldsymbol{u}. \tag{7}$$

This equation is found to express the relation between the incremental end-load vector and the incremental end-displacement one. Namely, a matrix $\boldsymbol{k}(\boldsymbol{u}, \Delta\boldsymbol{u})$ is the so-called chordal stiffness matrix of the member. If the increment of the member's rotation angle is small enough, this chordal stiffness matrix appears to give required accuracy. Then, by neglecting $\Delta\boldsymbol{u}$, this matrix is simply checked for agreement with the tangential stiffness matrix. Similarly, the chordal stiffness matrix of the entire structure, $\tilde{K}(X(t), \Delta X(t))$, is evaluated by summarizing the matrix $\tilde{\boldsymbol{k}}(\boldsymbol{u}, \Delta\boldsymbol{u})$ of all the members, as multiplied by each coordinate transformation matrix $\boldsymbol{c}(X(t))$. But, it should be noted that the increment $\Delta X(t)$ of the initial nodal displacement vector $X(t)$ is generally unknown at the beginning of the incremental step.

IV. PIECEWISE LINEARIZATION PROCEDURE

Using the initial internal resisting force vector $R(X(t))$ and the chordal stiffness matrix $\tilde{K}(X(t), \Delta X(t))$ derived in the above chapter, four different piecewise linearization procedures are newly proposed or reviewed for solving the non-linear equations of motion written by Eq. (1) in Chap. 2.

1) Incremental Form of Equations of Motion

To carry out a numerical step-by-step integration, it is necessary that the equations of motion be formulated in the incremental form. Furthermore, by applying a piecewise linearization technique, the incremental form of Eq. (1) is linearized as follows:

$$M \cdot \Delta\ddot{X}_{D,n+1} + \tilde{K}(X_s + \sum_{i=1}^{n} \Delta X_{D,i}) \cdot \Delta X_{D,n+1} = \Delta F_D(t_{n+1}) \tag{8}$$

where $\Delta\ddot{X}_{D,n+1}$ and $\Delta X_{D,n+1}$ are incremental nodal acceleration and displacement vectors caused by an incremental externally applied dynamic force vector $\Delta F_D(t_{n+1})$ at the $(n+1)$ -th incremental time step, respectively. And X_S is a nodal displacement vector caused by an externally applied static force vector F_S.

The left-hand second term of this equation is the one corresponding to a linearized increment or an internal resisting force vector. Namely, a matrix $\vec{K}(X_S + \sum_{i=1}^{n} \Delta X_{D,i})$ is a linearized stiffness matrix to be evaluated by conditions at the beginning of the incremental time step.

2) Linearized Stiffness Matrix

According to various forms for the above-mentioned linearized stiffness matrix, the piecewise linearization technique described herein can be classified into the following four methods:

(1) Chordal Stiffness Method (CSM)

$$\vec{K}(X_S + \sum_{i=1}^{n} \Delta X_{D,i}) = \tilde{K}(X_S + \sum_{i=1}^{n} \Delta X_{D,i}, \Delta X^*_{D,n+1}) \tag{9}$$

where

$$\begin{aligned}\Delta X^*_{D,n+1} &= \Delta X_{D,n} = 2\Delta X_{D,n} - \Delta X_{D,n-1},\\ &= 3\Delta X_{D,n} - 3\Delta X_{D,n-1} + \Delta X_{D,n-2},\\ &= 3\Delta X_{D,n} - 4\Delta X_{D,n-1} + 3\Delta X_{D,n-2} - \Delta X_{D,n-3},\\ &= \cdots\cdots\cdots\cdots\cdots\cdots\cdots\end{aligned}$$

(2) Tangential Stiffness Method (TSM)

$$\vec{K}(X_S + \sum_{i=1}^{n} \Delta X_{D,i}) = \tilde{K}(X_S + \sum_{i=1}^{n} \Delta X_{D,i}, 0) \tag{10}$$

(3) Additional Pseudoloads Method (APM)

$$\vec{K}(X_s + \sum_{i=1}^{n} \Delta X_{D,i}) \cdot \Delta X_{D,n+1} = \tilde{K}(X_s, 0) \cdot \Delta X_{D,n+1} + \Delta N^*_{D,n+1} \tag{11}$$

where

$$\begin{aligned}\Delta N^*_{D,n+1} &= \Delta N_{D,n} = 2\Delta N_{D,n} - \Delta N_{D,n-1},\\ &= 3\Delta N_{D,n} - 3\Delta N_{D,n-1} + \Delta N_{D,n-2},\\ &= 3\Delta N_{D,n} - 4\Delta N_{D,n-1} + 3\Delta N_{D,n-2} - \Delta N_{D,n-3},\\ &= \cdots\cdots\cdots\cdots\cdots\cdots\cdots\end{aligned}$$

$$\Delta N_{D,n} = R(X_S + \sum_{i=1}^{n} \Delta X_{D,i}) - R(X_S + \sum_{i=1}^{n-1} \Delta X_{D,i}) - \tilde{K}(X_S, 0) \cdot \Delta X_{D,n}.$$

(4) Linearized Stiffness Method (LSM)

$$\tilde{K}(X_s + \sum_{i=1}^{n} \Delta X_{D,i}) = \tilde{K}(X_s, 0). \tag{12}$$

In these equations, the contents of a matrix $\tilde{K}$ or a vector R is the same as the chordal stiffness matrix or the initial internal resisting force vector in the above chapter, respectively.

The method CSM in connection with an approximated chordal stiffness matrix seems to be proposed probably for the first time by the present study. From every reason, this method is expected to give a high degree of accuracy, comparing with the usual method TSM, and to enable highly rational reduction of an operating time on account of the decrease of a total number of incremental time steps, corresponding to the diminution of accumulation of numerical errors due to linearization. Moreover, comparing with the modified stiffness method by J. H. Argyris et al., it is obvious that this method will give a high degree of accuracy and efficiency in a numerical computation process.

On the other hand, the third and fourth methods, APM and LSM, apparently enable to apply a mode superposition besides a direct integration. Whence, as a quick and convenient method although incompletely accurate, these methods are expected to display their abilities in some cases, for example, systems with small nonlinearities and ones with a static load which forms a high ratio of its total loads.

3) Residual Force Vector

A residual force vector $Re(t_n)$, given by

$$Re(t_n) = F_S + \sum_{i=1}^{n} \Delta F_D(t_i) - M \cdot \sum_{i=1}^{n} \Delta \ddot{X}_{D,i} - R(X_S + \sum_{i=1}^{n} \Delta X_{D,i}) \tag{13}$$

is a measure to judge how well equilibrium condition is satisfied at a time t_n. In order to satisfy equilibrium condition up to a required tolerance at the end of each incremental time step, it may be necessary to use iterations.

On the occasion of using a piecewise linearization technique, this residual force vector $Re(t_n)$ is usually added to an incremental externally applied force vector $\Delta F_D(t_{n+1})$ at the next, namely, $(n+1)$-th incremental time step. However, because an operating time needed for evaluating this residual force vector occupies a rather high rate of its total operating time, it may be said that its addition is one of the largest trouble.

For this reason, if the accuracy of a linearized stiffness matrix makes it possible to prevent excess accumulation of numerical errors without considering the residual force vector, by using a time-increment smaller than a value needed not to produce immoderate truncation errors due to interpolation of an inertia force, the effect on reduction of a total operating time by a piecewise linearization technique can become even greater.

V. NUMERICAL EXAMPLES

1) Cantilever Beam with Static Load

In order to justify the proposed approximated chordal stiffness matrix, a cantilever beam subjected to a static load as illustrated in Fig. 2 is calculated in this section. To its

numerical calculation, an ordinary incremental method for a static large-deformation analysis by using a tangential stiffness matrix, as well as by using the proposed approximated chordal stiffness matrix, is applied. By comparing the results by the two methods with the ones converged by the Newton-Raphson iteration at every incremental step, accuracy of the proposed approximated chordal stiffness matrix will be examined.

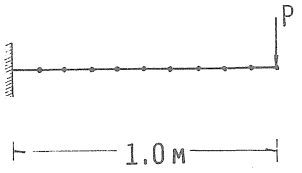

Fig. 2. Cantilever beam.

a) Conditions for numerical calculation (input data)

The cantilever beam is divided into ten and a vertical concentrated static load P applied at the free end is increased with a constant increment 1.0 t up to 10.0 t.

The following values are used for a sectional area, A, a moment of inertia of the members, I, and a Young's modulus of their material, E,:

$$A = 0.0001\,\mathrm{m}^2, \qquad I = 0.000001\ \mathrm{m}^4, \qquad E = 2.1 \times 10^7\ t/\mathrm{m}^2.$$

On the other hand, in the Newton-Raphson iteration, allowable errors in a convergence criterian, ε_d and ε_f for displacements and forces, respectively, are specified as $\varepsilon_d = \varepsilon_f = 10^{-5}$ at every incremental step.

b) Results of calculation (output data)

According to various methods, relative accumulation errors in vertical displacements at the free end at each incremental step in comparison with converged values are shown in Table 1 and, for reference, the number of iterations by the Newton-Raphson iteration is added to this table, in which a suffix * indicates a value calculated without considering a residual force vector.

Table 1. Relative Accumulation Errors in Vertical Displacements at Free end According to Various Methods.

Step No.	Calculation method				Converged value	No. of iter.
	Tangential	stiffness	Chordal	stiffness		
2	0.00662*	0.00347	0.00568*	0.00347	0.03171	4
4	0.01028*	0.00127	0.00791*	0.00079	0.06324	5
6	0.01610*	0.00053	0.00731*	0.00032	0.09439	4
8	0.02120*	0.00024	0.00600*	0.00024	0.12501	5
10	0.02530*	0.00013	0.00400*	0.00013	0.15493	10

2) Two-hinged Parabolic Arch Subjected to Moving Load

For justification of the methods proposed, a two-hinged parabolic arch subjected to a uniformly distributed moving load as illustrated in Fig. 3 is calculated. The results are com-

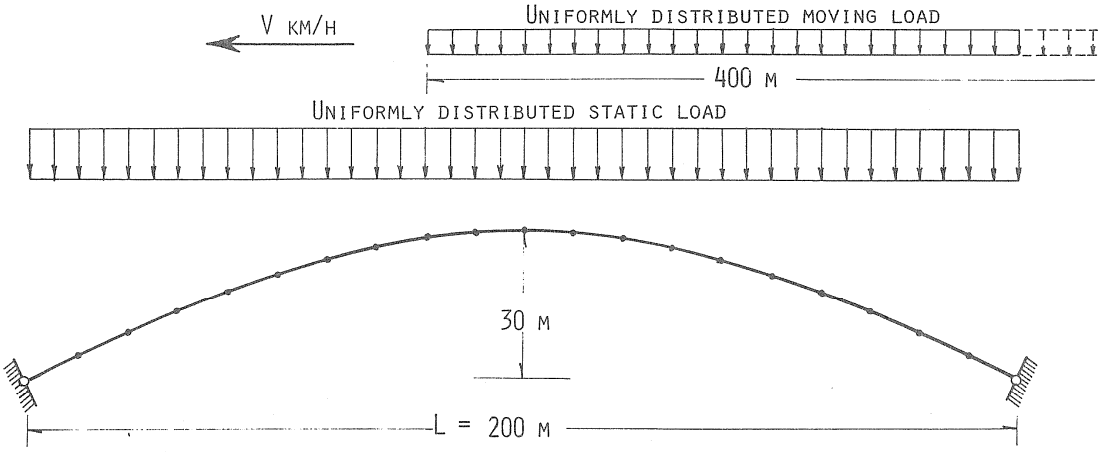

Fig. 3. Two-hinged parabolic arch.

pared with the ones, classified as "EXACT", converged by the Newton-Raphson iteration at every incremental time step. As numerical analysis techniques for a step-by-step integration and for an eigen-value problem expressed in terms of large order banded matrices, the well-known Newmark's β-method and the combined Sturm sequence method by K. K. Gupta are adopted.

a) Conditions for numerical calculation (input data)

The two-hinged parabolic arch is divided into twenty and the intensity of a uniformly distributed static load corresponding to the own weight of the members is 12.5 t/m.

At a speed V of a uniformly distributed moving load, 5.0 t/m, two cases, 160 km/h and 80 kgm/h, are performed.

The following values are used for a sectional area, A, a moment of inertia of the members, I, and a Young's modulus of their material, E,:

$$A = 0.5 \text{ m}^2, \qquad I = 0.5 \text{ m}^4, \qquad E = 2.1 \times 10^7 \ t/\text{m}^2.$$

Not to produce relative truncation errors greater than 0.01, four time-increments, $\Delta t =$ 0.03 sec, 0.04 sec, 0.05 sec and 0.06 sec, are used. But in the case of the speed $V = 80$ km/h, only one time-increment $\Delta t = 0.06$ sec is used. And a value of β in the Newmark's β-method is 0.25.

On the other hand, in the Newton-Raphson iteration, allowable errors in a convergence criterion, ε_d and ε_f for displacements and forces, respectively, are specified as $\varepsilon_d = \varepsilon_f = 10^{-4}$ at every incremental time step.

b) Results of calculation (output data)

According to various methods, relative accumulation errors in maximum vertical displacement in comparison with "EXACT" values are shown in Table 2, in which a suffix*

indicates a value calculated without considering a residual force vector. And in the case of the speed $V = 160$ km/h, relative accumulation error versus time-increment diagram is shown in Fig. 4.

Table 2. Relative Accumulation Errors in Maximum Vertical Displacements According toVarious Methods.

Speed (km/h)	Time-increment (sec)	"EXACT" values (m)	Calculation method			
			Direct integration		Mode superposition	
			CSM	TSM	APM	LSM
160	0.03	1.1842	0.0019* 0.0001	0.0996* 0.0001	0.1587* 0.1587	0.3360* 0.1792
	0.04	1.1856	0.0038* 0.0002	0.1314* 0.0002	0.1590* 0.1590	0.3356* 0.1856
	0.05	1.1838	0.0053* 0.0002	0.1594* 0.0004	0.1577* 0.1577	0.3337* 0.1925
	0.06	1.1877	0.0073* 0.0004	0.1916* 0.0007	0.1604* 0.1604	0.3327* 0.2003
80	0.06	0.5744	0.0008* 0.0001	0.0322* 0.0001	0.0629* 0.0629	0.2097* 0.0894

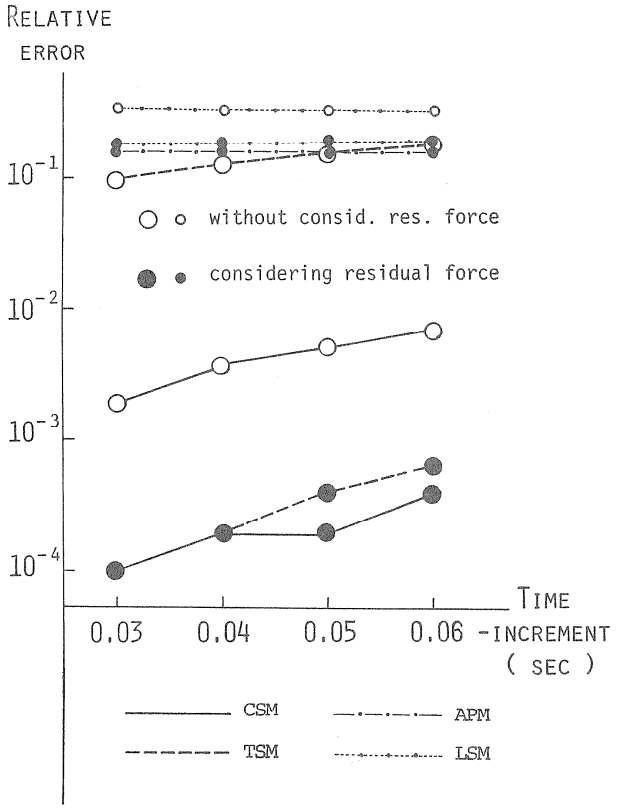

Fig. 4. Relative accumulation error versus time-increment diagram. ($V = 160$ km/h)

Figure 5 and Fig. 6 are vertical displacement versus time diagrams at $l/4$ point for the time-increment $\Delta t = 0.06$ sec in the two cases of the speeds $V = 160$ km/h and 80 km/h, according to various methods without considering a residual force vector. In which curves classified as 'STATIC' are the ones calculated by neglecting the effect of an inertia force.

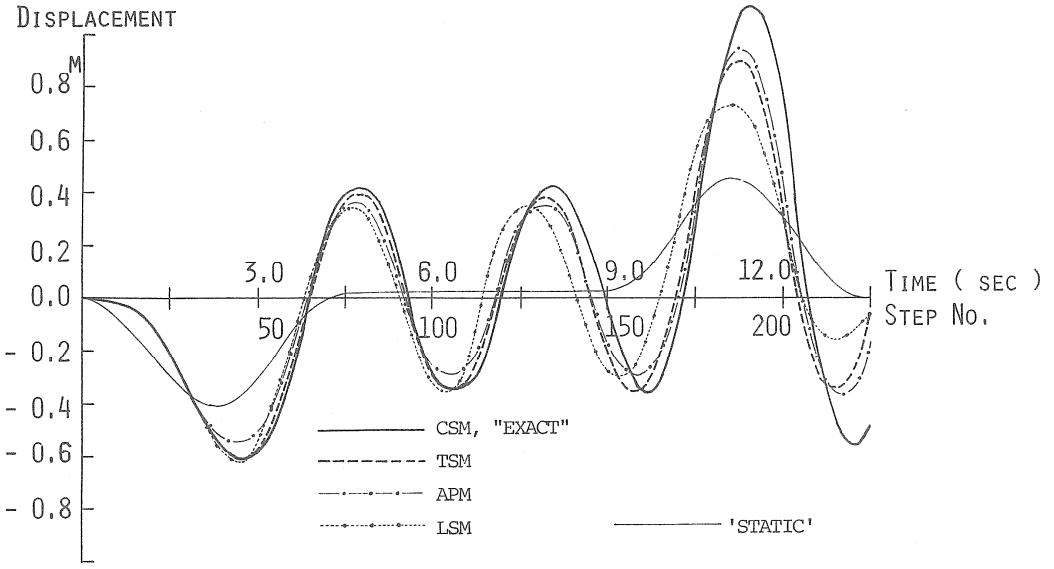

Fig. 5. Vertical displacement versus time diagram at $L/4$ point without considering residual force. ($V = 160$ km/h, $\Delta t = 0.06$ sec)

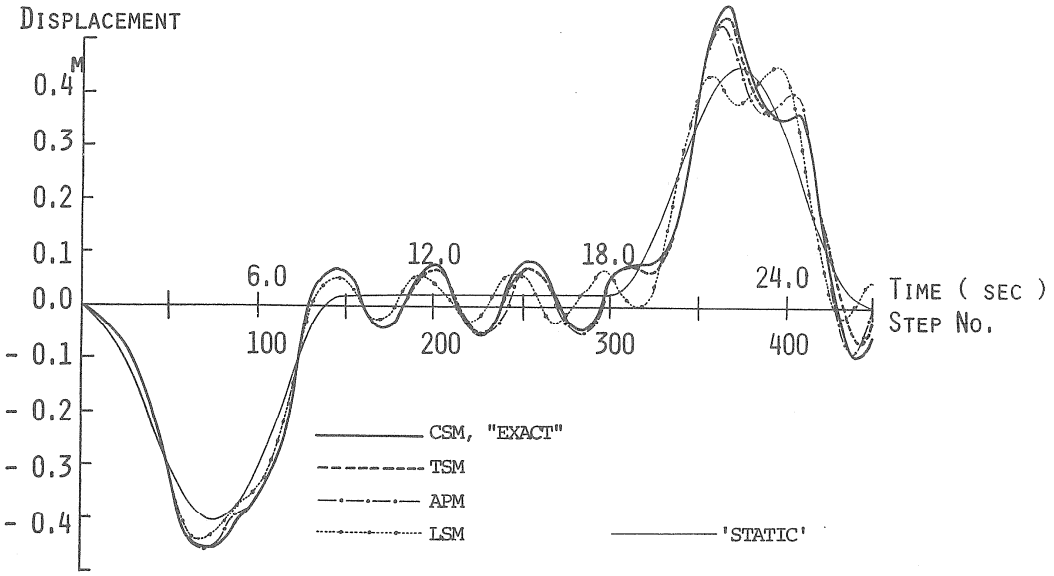

Fig. 6. Vertical displacement versus time diagram at $L/4$ point without considering residual force. ($V = 80$ km/h. $\Delta t = 0.06$ sec)

Furthermore, as the most important criterion for practice, the total operating time for the time-increment $\Delta t = 0.06$ sec in the case of the speed $V = 80$ km/h, according to various methods, is shown in Table 3, in which a suffix * is the same as the above one.

Table 3. Total Operating Time According to Various Methods.
($V = 80$ km/h, $\Delta t = 0.06$ sec)

"EXACT"	Calculation method			
	CSM	TSM	APM	LSM
7′10″	2′05″*	2′01″*	0′58″*	0′26″*
	2′34″	2′30″	1′02″	0′59″

VI. CONCLUSION

From the results of numerical examples, the following conclusions may be drawn:

(1) Although the difference of the total operating time between the two methods is hardly recognized, the method CSM, newly proposed by the present study, satisfies high accuracy by adding the residual force vector in comparison with the usual method TSM.

(2) In the method CSM, the accuracy of the approximated chordal stiffness matrix enables to prevent excess accumulation of numerical errors due to linearization without considering a residual force vector, by using a time-increment smaller than a value needed not to produce immoderate truncation errors due to interpolation of an inertia force.

(3) From the practical point of view, the methods CSM and TSM are quick in calculation and accurate enough for the non-linear vibration analysis of actual plane framed structures.

Particularly, the method CSM without considering a residual force vector is the most economical one because a total operating time of this method can be reduced to about 80% of the one of the usual method TSM, unless a band-width of the approximated chordal stiffness matrix increases to a considerable number.

(4) The methods APM and LSM are highly quick and convenient methods although incompletely accurate. These methods are expected to display their abilities in some cases, for example, systems with small nonlinearities and the ones with a static load which form a high ratio of its total loads.

REFERENCES

1) Argyris, J. H. et al., *Computer Meth. in Appl. Mech. and Engin.*, 2 (1973).
2) Clough, R. W., *Jap.-U.S. Semi. on Matrix Meth. of St. Anal. and Des.* (1969).
3) Wilson, E. L. et al., *Earthquake Engin. and St. Dyna.*, Vol. 1 (1973).
4) Stricklin, J. A. et al., *AIAA J.*, Vol. 9, No. 4 (1971).
5) Nickel, R. E., *U.S.-Jap. Semi. on Matrix Meth. of St. Anal. and Des.* (1972).
6) Nakao, Y. et al., *Proc. of the 1973 Tokyo Semi. on FEM* (1973).
7) Newmark, N. M., Proc. of ASCE, EM3 (1959).
8) Goudreau, G. L. et al., Computer Meth. in Appl. Mech. and Engin., 2 (1972).
9) Gupta, K. K., *Int. J. for Numerical Meth. in Engin.*, Vol. 7 (1973).

APPENDIX

Matrix $\boldsymbol{k}_{11}(\boldsymbol{u}, \Delta\boldsymbol{u})$:

$$\boldsymbol{k}_{11} = \begin{pmatrix} 0 & 0 & 0 & 0 & 0 & 0 \\ & A & B & 0 & -A & C \\ & & E & 0 & -B & D \\ & & & 0 & 0 & 0 \\ & \text{SYMM.} & & & A & -C \\ & & & & & F \end{pmatrix}$$

where

$$A = \frac{9EA}{35l_0^2}\{3(\tau_a + \tau_b)(\Delta v_a - \Delta v_b) + \tau_a \cdot \Delta\theta_a \cdot l_0 + \tau_b \cdot \Delta\theta_b \cdot l_0\},$$

$$B = \frac{3EA}{140l_0}\{12\tau_a(\Delta v_a - \Delta v_b) - (\tau_a - \tau_b) \cdot \Delta\theta_a \cdot l_0 + (\tau_a + \tau_b) \cdot \Delta\theta_b \cdot l_0\},$$

$$C = \frac{3EA}{140l_0}\{12\tau_b(\Delta v_a - \Delta v_b) + (\tau_a + \tau_b) \cdot \Delta\theta_a \cdot l_0 + (\tau_a - \tau_b) \cdot \Delta\theta_b \cdot l_0\},$$

$$D = \frac{EA}{140}\{3(\tau_a + \tau_b)(\Delta v_a - \Delta v_b) - (3\tau_a - 2\tau_b) \cdot \Delta\theta_a \cdot l_0 + (2\tau_a - 3\tau_b) \cdot \Delta\theta_b \cdot l_0\},$$

$$E = \frac{EA}{140}\{-3(\tau_a - \tau_b)(\Delta v_a - \Delta v_b) + 3(8\tau_a - \tau_b) \cdot \Delta\theta_a \cdot l_0 - (3\tau_a - 2\tau_b) \cdot \Delta\theta_b \cdot l_0\},$$

$$F = \frac{EA}{140}\{3(\tau_a - \tau_b)(\Delta v_a - \Delta v_b) + (2\tau_a - 3\tau_b) \cdot \Delta\theta_a \cdot l_0 - 3(\tau_a - 8\tau_b) \cdot \Delta\theta_b \cdot l_0\}.$$